Author Manuscript

Author Manuscript

Author Manuscript

Author Manuscript

HHS Public Access

Author manuscript

FASEB J. Author manuscript; available in PMC 2022 August 01.

Published in final edited form as:

FASEB J. 2021 August ; 35(8): e21770. doi:10.1096/fj.202100304R.

Constitutive expression of Steroidogenic factor-1 (NR5A1) disrupts ovarian functions, fertility and metabolic homeostasis in female mice

Emmi Rotgers[#1], **Barbara Nicol**[#1], **Karina Rodriguez**[1], **Saniya Rattan**[2], **Jodi A. Flaws**[2], **Humphrey Hung-Chang Yao**[1,*]

[1]Reproductive Developmental Biology Group, National Institute of Environmental Health Sciences, Research Triangle Park, NC, 27709, USA

[2]Department of Comparative Biosciences, College of Veterinary Medicine, University of Illinois, 2001 S. Lincoln Ave, Urbana, IL 61802

[#] These authors contributed equally to this work.

Abstract

Steroid hormones regulate various aspects of physiology, from reproductive functions to metabolic homeostasis. Steroidogenic factor-1 (NR5A1) plays a central role in the development of steroidogenic tissues and their ability to produce steroid hormones. Inactivation of *Nr5a1* in the mouse results in a complete gonadal and adrenal agenesis, absence of gonadotropes in the pituitary and impaired development of ventromedial hypothalamus, which controls glucose and energy metabolism. In this study, we set out to examine the consequences of NR5A1 over-expression (NR5A1+) in the NR5A1-positive cell populations in female mice. Ovaries of NR5A1+ females presented defects such as multi-oocyte follicles and an accumulation of corpora lutea. These females were hyperandrogenic, had irregular estrous cycles with persistent metestrus and became prematurely infertile. Furthermore, the decline in fertility coincided with weight gain, increased adiposity, hypertriglyceridemia, hyperinsulinemia and impaired glucose tolerance, indicating defects in metabolic functions. In summary, excess NR5A1 expression causes hyperandrogenism, disruption of ovarian functions, premature infertility, and disorders of metabolic homeostasis. This NR5A1 overexpression mouse provides a novel model for studying not only the molecular actions of NR5A1, but also the crosstalk between endocrine, reproductive and metabolic systems.

Keywords

NR5A1; ovary; hyperandrogenism; infertility; metabolism

[*]Corresponding author: Humphrey H-C Yao, Reproductive Developmental Biology Group, National Institute of Environmental Health Sciences (NIEHS/NIH), 111 T.W. Alexander Dr, Mail Drop C4-10, Research Triangle Park, NC 27709, U.S.A, Tel: 984-287-4004, humphrey.yao@nih.gov.

Author contributions

HHCY, ER, BN and KR conceived the study; HHCY supervised the project; ER, BN and KR performed experiments for ovarian and reproductive aspects of the study and analyzed the data; ER and KR performed the metabolic studies and analyzed the data. SR and JAF performed the follicle counting experiments. ER, BN and HHCY wrote the manuscript. All authors read and approved of the final manuscript.

Conflict of interest

The authors declare no competing financial or non-financial interests.

Author Manuscript Author Manuscript Author Manuscript Author Manuscript

Introduction

Female reproductive functions rely on a tightly regulated production of hormones and timely communication within the hypothalamic-pituitary-gonadal axis. Defects in steroidogenic hormone production can impair follicular development, estrous cycle and fertility. Elevated levels of androgens are associated with the development of polycystic ovarian syndrome (PCOS). Polycystic ovarian syndrome is the most common endocrine disorder that affects women in reproductive age (6–20% incidence depending on the diagnosis criteria used) (1, 2). PCOS is characterized by hyperandrogenism, irregular cycles, defects in ovulation or infertility and polycystic ovaries (2, 3). PCOS is also associated with obesity, insulin resistance, and higher risk of developing type II diabetes and cardiovascular diseases. This is a complex syndrome with a broad spectrum of clinical presentation amongst women. While the exact pathogenesis of PCOS remains unclear, it is assumed that both genetic traits and environmental factors could contribute to the phenotype variability. Genetic predisposition to PCOS is thought to be partially mediated by enhanced steroidogenic activity in the ovary in response to stimulus, such as LH or insulin.

Steroidogenesis and development of gonads require the orphan nuclear receptor NR5A1 (nuclear receptor subfamily 5 group A member 1), also known as Steroidogenic factor 1 or SF-1 (4, 5). NR5A1 is crucial for the formation of steroidogenic tissues such as gonads and adrenals and important for the function of pituitary and hypothalamus (6–8). In the mouse, NR5A1 is expressed in somatic cells of undifferentiated gonads of both XX and XY embryos and loss of *Nr5a1* results in gonadal agenesis (6, 9). NR5A1 expression is maintained in differentiating testes, where it plays a key role as a co-factor of testis-determining factors SRY and SOX9 (10) as well as a master regulator of steroidogenesis (11). In the fetal ovary, on the other hand, NR5A1 expression is downregulated and will only be detected again close to birth, before follicles start to form (9). In the mature ovary, NR5A1 is expressed in theca cells, granulosa cells and luteal cells (12). In humans, mutations in *NR5A1* gene lead to disorders of sex development in both XX and XY individuals, with a wide spectrum of phenotypes, spanning from gonad dysgenesis, sex reversal, to reduced fertility (13). In XX individuals, mutations in *NR5A1* are associated with ovo-testicular development as well as primary ovarian insufficiency (14, 15). Beyond its role in gonad formation and differentiation, NR5A1 also plays key roles in ovarian physiology: granulosa-cell specific *Nr5a1* KO in postnatal ovary causes abnormal estrous cycles and infertility (16, 17). In differentiated steroidogenic cells, NR5A1 is a master regulator of steroidogenesis by controlling the expression of key steroidogenic enzymes and promoting cholesterol metabolism (4, 5, 11).

The functions of NR5A1 highlight the importance of a properly tuned expression of NR5A1 for gonad development as well as endocrine functions of the individual. In this study, we set out to investigate the consequences of increased NR5A1 expression on ovarian development, female fertility and metabolism by generating a mouse model that overexpresses NR5A1 specifically in the NR5A1-positive cell populations.

Author Manuscript Author Manuscript Author Manuscript Author Manuscript

Materials and Methods

Mouse models

To induce over-expression of NR5A1, Rosa26-LS*L-Nr5a1* $^{+/f}$ mice (18, 19) were mated with *Nr5a1-Cre*$^{Tg/+}$ mice (20). This strategy resulted in overexpression of NR5A1 specifically in cells that normally express NR5A1. The mouse genetic background was mixed C57BL/6/129SvEv. The presence of a Myc-tag fused in-frame to the 5' end of *Nr5a1* coding sequence allowed for the immuno-detection of NR5A1 specific of the transgene (18). For timed mating, noon on the day when the vaginal plug was observed was considered E0.5. All animal studies were conducted in accordance with the NIH Guide for the Care and Use of Laboratory Animals and approved by the National Institute of Environmental Health Science (NIEHS) Animal Care and Use Committee.

RNA extraction and quantitative real-time PCR

Total RNA was isolated from tissues using the Arcturus PicoPure RNA isolation kit (Thermo Fisher) for E16.5 (n=7/genotype) and newborn P0 ovaries (n=6/genotype). For adult tissues, total RNA was isolated using RNeasy Mini kit (Qiagen) (n=4–5/genotype for ovaries and hypothalami, n=8/genotype for pituitaries). RNA quality and concentration were determined using the Nanodrop 2000c. First-strand cDNA synthesis was performed using the Superscript II cDNA synthesis system using the manufacturer's protocol (Invitrogen). Gene expression was analyzed by real-time PCR using either SYBR green (Applied Biosystems) or Taqman (Bio-rad) assays. Taqman probes and primer sequences used in qPCR are listed in Supplemental Table 1. Cycle threshold (Ct) values were obtained using the Bio-Rad CFX96TM Real-Time PCR Detection system. The relative fold change of each transcript was normalized to *Gapdh* or *Rps29* as endogenous references.

Histological analysis, immunohistochemistry and immunofluorescence

Tissues from control and NR5A1+ females were collected fixed in 4% paraformaldehyde in PBS at 4°C from 2h to overnight. These samples were dehydrated through an ethanol gradient, embedded in paraffin wax and sectioned to 5 μm thickness. Slides were dewaxed and rehydrated in a series of decreasing gradients of alcohol. For immunohistochemistry, slides were pretreated in citric acid–based Antigen Unmasking Solution (Vector Labs) followed by blocking endogenous peroxidase activity using Bloxall Peroxodase Blocking solution (Vector Labs). Sections were blocked for 1 hour in blocking buffer composed of 5% normal donkey serum in PBS-Triton X-100 solution. Slides were then incubated with primary antibodies against either NR5A1 (1:500; a kind gift from Ken-ichirou Morohashi) or Myc-Tag (1:200; #71D10, Cell Signaling) in blocking buffer overnight at 4°C. The sections were then washed PBS-Triton X-100 and incubated for 1 hour in Biotin-SP-conjugated anti-Rabbit antibody (1:400; #711-066-152, Jackson Immuno Research) in blocking buffer. Signal was detected using the chromogenic Vector ABC kit coupled with HRP and DAB (Vector Labs) according to manufacturer's instructions. Slides were counterstained with Mayer's hematoxylin, dehydrated and embedded in Permount. For histological analysis, sections were stained with hematoxylin and eosin. Histological and immunohistochemical slides were scanned using an Aperio ScanScope XT Scanner (Aperio Technologies/Leica Microsystems) for digital image analysis. For immunofluorescence

Author Manuscript Author Manuscript Author Manuscript Author Manuscript

experiments, slides were pretreated in citric acid–based Antigen Unmasking Solution (Vector Labs) followed by blocking for 1 hour in blocking buffer. Slides were then incubated with primary antibodies against Myc-Tag, NR5A1 (1:200, KO610, CosmoBio), or CYP17A1 (1:100; sc-46081, Santa Cruz) in blocking buffer overnight at 4°C. The sections were then washed PBS-Triton X-100 and incubated for 1h in corresponding Alexa Fluor fluorescent secondary antibodies (Invitrogen) in blocking buffer. Slides were washed and incubated in quenching buffers TrueView (Vector Labs) and TrueBlack (Biotium) according to manufacturers' instructions to remove autofluorescence from blood cells and lipofuscin. Following counterstaining with DAPI, slides were mounted in ProLong Diamond Antifade Mountant (Invitrogen) and imaged under a Leica DMI4000 confocal microscope.

Follicle quantification

Follicles were quantified as described previously (21). Briefly, ovaries from P21, 3 and 7-month-old control and NR5A1+ mice were sectioned serially at 8μm and stained with hematoxylin and eosin. Follicle number were counted in every 10^{th} section. Follicles were classified as primordial follicles when only a single layer of squamous granulosa cells was present and as primary follicles when the single layer of granulosa cells was cuboidal. Pre-antral follicles correspond to follicles with at least two layers of cuboidal granulosa cells, and antral follicles in the presence of a fluid-filled antral space. Multi-oocyte follicles correspond to follicles with more than one oocyte. To avoid double counting, pre-antral and antral follicles were only counted when the nucleus was present. Corpora lutea (CL) were counted every 200 μm and the average number of CL per section was calculated for each ovary (n=4 ovaries/genotype/age).

Fertility Study and estrous cyclicity analysis

Control (n=8) and NR5A1+ (n=9) females were mated with males with proven fertility from 10-weeks (2 months) to 37 weeks of age (9 months). The litter size was recorded on the day of birth. Total number of litters and total number of pups per dam was recorded. The percentage of fertile females was determined based on the age of the last litter. Estrous cycle was monitored in 3- and 7-month-old females by flushing the vagina with 50 μl of sterile 0.9% NaCl daily for 18 consecutive days (n=8–9/genotype). Vaginal smears were immediately fixed on glass slides (Safetex; Andwin Scientific) and stained with hematoxylin and eosin (H&E). Phases of the estrous cycle were determined based on vaginal cytology as previously described (Cora et al., 2015). Females were considered cycling irregularly if they had less than 2 cycles over a period of 15 days.

Superovulation

Three-month old females (n=8 per genotype) were injected intraperitoneally with pregnant mare serum gonadotropin (PMSG, 5 IU; Calbiochem) followed by injection of human chorionic gonadotropin (hCG) 46 hours later (5 IU; Calbiochem). Animals were euthanized 14 hours after the hCG injection. Ovulated oocytes were collected from the ampulla of the oviduct and counted.

Author Manuscript Author Manuscript Author Manuscript Author Manuscript

Steroid hormones and gonadotropin assays

Serum from 7-month-old control and NR5A1+ female mice were collected (n= 6 per genotype) in metestrus and stored at −80°C prior to analyses. Serum levels of estradiol, progesterone, testosterone and androstenedione were measured using LC-MS/MS by the Pharmacology Department at University of Eastern Finland as described earlier (Häkkinen et al., 2018). Gonadotropins LH/FSH were analyzed by the University of Virginia Center for Research in Reproduction Ligand Assay and Analysis Core using the Pituitary Panel Multiplex kit (EMD Millipore), with a reportable range of 0.24–30.0 ng/mL for LH and 2.4 – 300.0 ng/mL for FSH, intra-assay CV of 5.1% and inter-assay CV of 9.6%. Serum from 3-month-old control and NR5A1+ females in proestrus (n=6 per genotype) were analyzed by the University of Virginia Center for Research in Reproduction Ligand Assay and Analysis Core. Competitive enzyme immunoassay ELISA was performed in duplicates to measure Testosterone (IB79174; IBL), Estradiol (ES180S-100; Calbiotech) and Progesterone (IB79183; IBL).

Body weight and body composition analysis

Body weight was measured at 1, 2, 3, 6, 8 and 12 months of age for control and NR5A1+ females (n= 10–16 per genotype). Body composition was assessed from 5-month-old control and NR5A1+ mice (n=8–9 per genotype) using an MRI-based device LF90 MiniSpec (Bruker).

Intraperitoneal glucose tolerance test

Adult female mice (5-month-old) were fasted for 6 hours in the morning (n= 8–9 per group). The mice were then given an intraperitoneal bolus of 2,000 mg/kg glucose in sterile 0.9M NaCl. Serum glucose level was measured from whole blood sampled via tail snip using Alphatrak 2 Veterinary Point-of-Care glucometer before and after 20, 40, 60 and 120 min of glucose administration.

Clinical chemistry assays

Seven-month-old control and NR5A1+ females (n=6 per genotype). were fasted for 8 h and sacrificed between 3–5 pm in the afternoon to minimize biological variability due to preanalytical factors. Sera were collected and frozen in −80C. Serum glucose and liver panel were measured on a Beckman Coulter Olympus AU 400e Clinical Chemistry Analyzer (Beckman Coulter Inc.) using reagents from the manufacturer Beckman Coulter. Adiponectin was measured using the adiponectin mouse ELISA kit and leptin and insulin were assayed with Mouse Metabolic Kit according to the manufacturer’s instructions (Meso Scale Discovery).

Statistical analyses

Statistical analyses were performed using the GraphPad Prism 7 software. Results are presented as the mean of biological replicates ± standard error of the mean (SEM). The normal distribution of biological replicates was determined using the Shapiro–Wilk test. Depending on whether the data had a normal distribution, statistical significance was tested using unpaired Student t-test or non-parametric Mann-Whitney test. Follicle quantification,

Author Manuscript Author Manuscript Author Manuscript Author Manuscript

estrous cycles, glucose tolerance test were analyzed by 2-way analysis of variance ANOVA. All values are presented as mean ± S.E.M. ns: non-significant; *: p<0.05; **: p<0.01; ***: p<0.001and ****: p<0.0001.

Results

Generation of NR5A1 overexpression model

To induce a constitutive over-expression of NR5A1 in the ovary, we took advantage of the *Rosa26-LSL-Nr5a1*$^{+/f}$ mice (18, 19), in which *Nr5a1* transgene expression is induced by the presence of Cre recombinase. By crossing it with *Nr5a1-Cre*$^{Tg/+}$ mice (20) (Fig. 1A), we specifically targeted cells that normally express NR5A1. The genotypes of the NR5A1 overexpressing mice (or NR5A1+ thereafter) and their control littermates were *Nr5a1-Cre*$^{Tg/+}$*; Rosa26-LSL-Nr5a1*$^{+/f}$ and *Nr5a1-Cre*$^{Tg/+}$*; Rosa26-LSL-Nr5a1*$^{+/+}$ *or Nr5a1-Cre*$^{+/+}$*; Rosa26-LSL-Nr5a1*$^{+/f}$, respectively. The biological outcome and phenotypes of these two controls were statistically identical. We first confirmed *Nr5a1* transgene expression in the NR5A1+ fetal ovary at E16.5 by RT-PCR (Fig. 1B). We also detected an increased expression of total *Nr5a1* that includes both endogenous *Nr5a1* and the transgene at E16.5, P0, P21, and 3 months (Fig. 1C). At birth or P0, when endogenous *Nr5a1* became upregulated (9), expression of total *Nr5a1* (endogenous + transgene) was 2 times higher in NR5A1+ ovaries compared to control ovaries (Fig. 1C). Total *Nr5a1* expression tended to be higher in NR5A1+ ovaries at P21, albeit not statistically significant, and was significantly higher in NR5A1+ ovaries at 3 months of age (Fig. 1C). To identify the cellular location of NR5A1 expression coming from the transgene in the ovary, we performed immunohistochemical detection for both MYC Tag (specific to the transgene) and NR5A1 protein (Fig. 1D–E). While no MYC tag expression was detected in control ovaries at any time, some somatic cells were MYC+ in NR5A1+ ovaries at P0, 2 weeks, and 3 months of age (Fig. 1D). At P0, a few of these MYC+ cell presented a strong expression while most had a weak MYC expression (insets in Fig. 1D). This difference likely represented the two waves of NR5A1 expression, with the strong MYC+ cells representing cells for which the transgene was induced several days ago in the undifferentiated gonads and the weak MYC+ cells representing the cells for which the transgene was only induced close to birth. At 2 weeks of age (2w), most somatic cells presented a strong MYC expression in NR5A1+ ovaries, particularly granulosa cells and theca cells (Fig. 1D, arrow and arrowhead). At 3 months of age (3m), in addition to its expression in granulosa and theca cells, MYC tag was detected in corpora lutea (Fig. 1D). As a consequence of NR5A1 expression from the transgene, NR5A1 protein staining appeared to be stronger in NR5A1+ ovaries at P0 compared to control ovaries (Fig. 1E). NR5A1 protein was only weakly detected in somatic cells of control newborn ovaries as a result of its recent neonatal activation (9). In 2-week-old ovaries, no clear difference was observed in NR5A1 expression as the pattern of NR5A1 transgene expression followed that of the endogenous NR5A1 at this age (Fig. 1D–E). At 3 months, a clear difference in NR5A1 expression pattern appeared, with a stronger expression in corpora lutea of NR5A1+ ovaries compared to control ovaries (Fig. 1E, inset). These results indicated that our mouse model resulted in a mild over-expression of NR5A1 in somatic cells of the ovary where most of the *Nr5a1* transgene activation occurred neonatally and postnatally as folliculogenesis starts.

Author Manuscript Author Manuscript Author Manuscript Author Manuscript

Overexpression of NR5A1 leads to ovarian defects

Histological analyses of the ovaries at P21 revealed the increased presence of multi-oocyte follicles (MOF) in NR5A1+ ovaries (Fig. 2A, arrowheads). While follicle quantification at P21 did not show any significant difference in the number of primordial, primary, preantral and antral follicles (Fig. 2B), the number of MOF was 6 times higher in NR5A1+ than control ovaries (Fig. 2C). The number of MOF also tended to be higher at 3m and 7m, although not statistically significant (Fig. 2C; Fig. D arrowheads). The most apparent morphological change in the NR5A1+ ovaries was the increased presence of corpora lutea (CL) at 3m (Fig. 2D, asterisks) and at 7m (Fig. S1A). The number of CL was significantly higher in NR5A1+ ovaries and increased overtime (Fig. 2E). This CL accumulation led to an increase in ovarian size and the NR5A1+ ovaries were twice as heavy and large as the control ovaries at 7-month-old (Fig. 2F and Fig. S1A). Gene expression analyses revealed that genes expressed in hormonally active CL, such as *Star* and prolactin receptor (*Prlr*), were strongly upregulated, likely due to the high number of CL present in the ovary. Similarly, there was a strong upregulation in expression of genes involved in CL functional regression, such as *Ptgfr*, and *Akr1c18*, encoding 20αHSD, the enzyme that catabolizes progesterone (Fig. S1A), suggesting that the accumulated CL would eventually become hormonally inactive. On the other hand, there was no upregulation of genes involved in the structural regression of CL, i.e. luteal cell death, despite the large number of CL present. For instance, *Tnfr2* was significantly downregulated, while *Fas* expression was similar to control ovaries (Fig. 2G). Similar phenotype of CL accumulation associated with impaired structural regression was observed in *Inhba/Inhbb* double knockout ovaries (22). Interestingly, both *Inhba* and *Inhbb* were strongly downregulated in NR5A1+ ovaries (Fig. S1B), suggesting a role of Activins in CL structural regression. Taken together, NR5A1 overexpression leads to progressive accumulation of corpora lutea in adult ovaries due to impaired structural regression of luteal cells.

NR5A1+ females exhibit impaired fertility and abnormal estrus cycles

Next, we examined whether overexpression of NR5A1 in NR5A1+ cells affected female fertility (Fig. 3A). Ten-week-old control and NR5A1+ females were mated with control males until the females reached the age of 9 months (n=8 controls and n=9 NR5A1+ females). While the time to first litter was not significantly different between control and NR5A1+ females (Fig. S1C), fertility of NR5A1+ females progressively declined over the testing period. By the age of 25 weeks (5.5 months), 50% of NR5A1+ females already became infertile and by 34 weeks (8 months), only 30% of NR5A1+ females remained fertile (Fig. 3A). The mean litter size was comparable between NR5A1+ and control females, but the mean number of litters per female and consequently the cumulative number of pups per female were significantly lower in the NR5A1+ females (Fig. 3B). At the end of the fertility study, ovarian histology was performed to compare the ovarian phenotype of control females, NR5A1+ females that had a litter within a month of the end of the study (“fertile”), and NR5A1+ females that stopped breeding early on (“infertile”). NR5A1+ ovaries tended to be larger than control ovaries, particularly those of females that became infertile early on. Ovaries from infertile females still contained growing follicles, indicating that the loss of fertility was not caused by an exhaustion of the ovarian reserve (Fig. 3C). However, these ovaries contained retained oocytes surrounded by luteinized cells, suggesting

Author Manuscript Author Manuscript Author Manuscript Author Manuscript

an ovulatory dysfunction and premature luteinization of granulosa cells (Fig. 3C arrowheads and insets).

To determine whether the decline in fertility could be a result of endocrine dysfunction and impaired estrus cyclicity, we monitored estrous cycles in 3m old control and NR5A1+ females (Fig. 3D). NR5A1+ females spent significantly longer time in metestrus and less time in estrus (Fig. 3D & E). At 3m, 25% of NR5A1+ females exhibited irregular cycles, defined by less than 2 cycles over a period of 15 days (Fig. 3F). By 7m, this number rose to 45% of NR5A1+ females. Normal estrous cycles rely on timely communication between hypothalamus, pituitary and ovary. To determine whether NR5A1+ females had ovulation defects, we performed superovulation experiments on 3-month-old females, an age for which some NR5A1+ females start to present changes in their estrous cycle (Fig. 3D). However, the mean number of ovulated eggs was not significantly different between control and NR5A1+ females (Fig. S1D). Administration of exogenous gonadotropins allowed us to bypass the hypothalamus-pituitary signaling to the ovary in order to induce superovulation. The hypothalamus and pituitary are both targets of *Nr5a1-Cre* and the transgene expression was induced in both tissues (Fig. S2A–D). Despite significant upregulation of *Nr5a1* in both tissues, gene expression analysis in hypothalamus and pituitary of 3-month-old females in proestrus showed no significant change of expression for key endocrine-related genes. For instance, expression of gonadotropin releasing hormone 1 (*Gnrh1*) and Kisspeptin 1 (*Kiss1*) in the hypothalamus (Fig. S2B) and follicle stimulating hormone subunit beta (*Fshb*) in the pituitary (Fig. S2D) was not significantly changed, although all three genes tended to show lower expression in NR5A1+ females. Meanwhile, luteinizing hormone subunit beta *Lhb* was significantly downregulated in NR5A1+ pituitaries. However, no difference in gonadotropin serum levels was detected at 7m (Fig. S2F). Gene expression analyses in both 3m and 7m ovaries showed that *Fshr*, encoding FSH receptor, was significantly downregulated in NR5A1+ ovaries, suggesting that NR5A1+ ovaries may not fully respond to FSH signal from the pituitary (Fig. S2E). On the other hand, *Lhcgr*, encoding LH receptor, was not changed. In summary, NR5A1+ females have increased numbers of multi-oocyte follicles at P21 and accumulation of CL in mature ovaries, and developed progressive infertility associated with abnormal estrous cycles.

NR5A1+ females become hyperandrogenic

NR5A1 is known to be a key regulator of steroidogenesis (4, 5, 11); therefore, we examined whether NR5A1 overexpression altered steroidogenic gene expression in the ovary and hormone production (Fig. 4 and Fig. S3). Expression of *Star*, *Cyp11a1* and *Cyp17a1* was not significantly changed at birth and P21 (Fig S3A–B). In 3m proestrus NR5A1+ ovaries, expression of steroidogenic genes was not significantly changed apart from *Star,* which was strongly upregulated (Fig. S3C). Serum levels of testosterone and estradiol tended to be higher in 3m old NR5A1+ females in proestrus, although not significantly (Fig. S3D). Meanwhile, progesterone levels were significantly higher, likely due to the increased presence of CL. At 7m old, an age for which many NR5A1+ females have cycle irregularities and fertility issues (Fig. 3), steroidogenic genes *Star*, *Cyp11a1* and *Hsd3b1* were upregulated (Fig. 4A). In addition, *Hsd17b3*, which is normally expressed in the testis and converts androstenedione into testosterone, was significantly upregulated in NR5A1+

Author Manuscript Author Manuscript Author Manuscript Author Manuscript

ovaries. Along with this upregulation of multiple steroidogenic genes, the levels of testosterone and androstenedione were significantly elevated in the 7m NR5A1+ mice in metestrus compared to the controls (Fig. 4B). Serum progesterone in NR5A1+females was also increased compared to the controls, albeit not statistically significant. As expected in metestrus, estradiol levels were very low in control females. Despite high levels of androgens, NR5A1+ females had similar levels of estradiol to controls (Fig. 4B). While there was no significant change in *Cyp17a1* gene expression in adult NR5A1+ ovaries (Fig 4A and S3), immunofluorescence for CYP17A1 revealed abnormal distribution of CYP17A1+ cells in NR5A1+ ovaries (Fig. 4C). In 3m and 9m old control ovaries, CYP17A1 was exclusively expressed in the theca layer surrounding growing follicles (arrowheads). While CYP17A1 was detected in theca cells of 3m NR5A1+ ovaries, it was not the case anymore at 9m of age. Moreover, a few CYP17A1+ cells were present in the interstitium of 3m NR5A1+ ovaries (arrowhead), and by 9m, the interstitium became the main source of CYP17A1. Altogether, these results indicated that adult NR5A1+ females progressively developed hyperandrogenism, likely caused by the abnormal appearance of steroidogenic cells in the interstitium.

NR5A1+ females become overweight and present metabolic defects

Hyperandrogenism in females is often associated with impaired metabolic functions and occurs in women suffering from polycystic ovarian syndrome and in post-menopausal women (23). By the age of 6 months, NR5A1+ females were significantly heavier than their control littermates and this weight gain continued as the mice aged (Fig. 5A–B). Analyses of body composition by MRI-based scanner revealed that the body fat percentage was significantly higher in 5m NR5A1+ females compared to controls (Fig. 5C). Both perigonadal fat pads and retroperitoneal fat were significantly heavier in 7m NR5A1+ females compared to control females (Fig. 5D).

We next examined serum levels of leptin and adiponectin to gain insight into the endocrine aspects of weight gain (Fig. 6A). Consistent with the increased body fat percentage, serum levels of leptin, produced by adipocytes, were increased over 20-fold in 7m fasting NR5A1+ females compared to the controls. On the other hand, serum levels of adiponectin, which is also produced by adipocytes, remained unchanged in NR5A1+ females (Fig.6A). To further assess potential insulin sensitivity, we measured serum levels of insulin and glucose in the fasting state (Fig. 6A). Fasting blood glucose was not altered in 7m NR5A1+ females; however, insulin was significantly elevated. In addition to the hyperinsulinemia phenotype, intraperitoneal glucose tolerance test on 5-month-old female mice revealed a mild impairment of glucose tolerance in NR5A1+ females compared to controls (Fig. 6B).

Metabolic syndrome and hyperandrogenism in mice are often coupled with hepatic steatosis (24). However, NR5A1+ female mice developed no signs of fatty liver disease: serum activities of liver enzymes alanine aminotransferase (ALT), aspartate aminotransferase (AST), Alkaline phosphatase (ALP) as well as serum level of total bile acid (TBA) at 7m and liver histology at 12m were not significantly different between NR5A1+ and control females (Fig. S4). Because hypertriglyceridemia is common in hyperandrogenism, we measured lipids in the serum. NR5A1+ females exhibited significantly elevated serum levels

Author Manuscript Author Manuscript Author Manuscript Author Manuscript

of triglycerides while total cholesterol, HDL and LDL levels were unchanged (Fig. 6C and Fig. S4). Taken together, the physiological phenotypes of NR5A1+ females, such as increased adiposity, impaired glucose tolerance, hyperinsulinemia and hypertriglyceridemia largely recapitulate the metabolic phenotype commonly associated with exposure to excess androgens in the female. However, increased androgen levels in these mice were not associated with liver steatosis and decreased adiponectin.

Discussion

In this study, we demonstrated that overexpression of NR5A1 impairs female reproductive functions and metabolic homeostasis (Fig. 6D). Ovaries of NR5A1+ females contained multi-oocyte follicles and accumulated corpora lutea. These NR5A1+ females had irregular cycles, became prematurely infertile, and were hyperandrogenic. Beyond the defects in reproductive functions, these females presented metabolic defects such as increased body weight, increased adiposity, hyperinsulinemia, hyperleptinemia, glucose intolerance and hypertriglycemia, which are features commonly observed in women with hyperandrogenic syndromes.

NR5A1 is required for the morphogenesis of the gonads (9) and loss- or gain-of-function mutations lead to disorders of sex development in both XX and XY individuals (25). XX individuals with a gain-of-function mutation of *NR5A1* developed ovo-testes instead of ovaries (14, 26); therefore, we suspected that our mouse model of NR5A1 overexpression could result in masculinization of XX fetal gonads. However, we did not observe such phenotype in the NR5A1+ females. *Nr5a1*-Cre mouse model has been extensively used by our lab and other labs to efficiently induce gene knockout or overexpression around the time of sex determination (20, 27–30). Nevertheless, in the NR5A1+ model that we generated, *Nr5a1* transgene induction was only partial in fetal gonads and most of the activation of *Nr5a1* transgene expression occurred in the neonatal and postnatal ovary (Fig.1C–E). It is therefore possible that overexpression of *Nr5a1* in this model occurred too late to impact sex determination of the embryonic gonads. Another possibility is that expression of *Nr5a1* alone is insufficient to masculinize the fetal mouse ovary. In fact, another model of *Nr5a1* overexpression in the mouse fetal ovary was recently generated by Nomura et al (31). In that study, the authors used a transgenic *Wt1*-BAC system, a strategy that targets somatic cells of the gonads at the time of sex determination (32). Similar to our findings, overexpression of *Nr5a1* in the mouse model by Nomura et al did not cause masculinization of XX gonads either, suggesting that NR5A1 alone is insufficient to masculinize mouse XX gonads, contrary to some human *NR5A1* mutations (14, 31). Ovaries from the model by Nomura *et al.* also had a significant increase in multi-oocyte follicles, and the authors showed that it was likely caused by impaired Notch signaling (31). Other than the multi-oocyte phenotype, however, the ovarian phenotypes in our model are drastically different from this study. Nomura et al reported that NR5A1+ females presented a significant decrease in antral follicle numbers and fertility was already compromised in young females. These discrepancies are likely caused by the differences in activation of *Nr5a1* transgene expression between the two models in terms of the timing of induction, the cell populations targeted (*Wt1*+ vs. *Nr5a1*+ cell populations) and the level of transgene expression.

Author Manuscript Author Manuscript Author Manuscript Author Manuscript

Unfortunately, there is no information regarding androgen levels in adult females, estrous cycles and potential metabolic aspects in the model by Nomura et al (31).

The constellation of phenotypes in our NR5A1 overexpression mouse model, irregular cycles, impaired fertility, increased body weight, hyperinsulinemia and other metabolic defects (Fig. 6D), could be attributed to hyperandrogenism. Androgen exposure can indeed alter endocrine homeostasis, resulting in both reproductive and metabolic dysfunctions (33). In our model, hyperandrogenism seem to appear relatively late, between 3 and 7m of age, which corresponds to the time mice develop irregular cycles, become overweight, and some of them become infertile. Similar to models of exogenic androgen exposure, NR5A1+ mice developed abnormal cycles, weight gain, increased adiposity, hyperinsulinemia, and glucose intolerance. However, NR5A1+ mice maintained normal adiponectin levels, which likely contributed to the relative metabolic health of the mice without liver steatosis despite obesity (34). Androgens can act directly through the androgen receptor (AR) as well as indirectly through its aromatized product estrogens via estrogen receptor (ER). Studies of testosterone and non-aromatizable dihydrotestosterone (DHT) treatments in control and AR knockout mice demonstrated that an indirect action of androgen through ER could contribute to reproductive defects such as irregular cycles (35). On the other hand, a direct action through androgen receptor was required to induce the metabolic defects, and global AR knockout can prevent the development of metabolic defects in mice exposed to DHT (35, 36). Our results support that excess androgen in our mouse model is directly due to NR5A1 overexpression in the ovary. NR5A1 can indeed directly control the expression of steroidogenic enzymes (5), and various steroidogenic enzymes, including known direct targets of NR5A1 (37), were significantly upregulated in the ovary, concomitant with the significant upregulation of androgen serum levels. Most surprisingly, NR5A1+ ovaries expressed *Hsd17b3*, a gene that is normally expressed in the Leydig cells of the testis where it permits the conversion of androstenedione into testosterone. Ectopic *Hsd17b3* expression was previously found in ovaries of αERKO mutant females, where it was associated with appearance of Leydig-like steroidogenic cells in the ovarian interstitium, and consequently, with hyperandrogenism (38). Here, we detected the growing presence of CYP17A+ steroidogenic cells in the interstitium of NR5A1+ ovaries, whereas in normal conditions CYP17A1 was only detected in theca cells surrounding growing follicles. This suggests the abnormal appearance of steroidogenic cells in the interstitium of the adult ovary that could contribute to the hyperandrogenism phenotype. Hyperandrogenism could also be secondary to hyperinsulinemia since insulin induces increased androgen production in theca cells (39). Obesity and hyperinsulinemia can exacerbate hyperandrogenism and reproductive and metabolic defects (40).

Hyperandrogenism is considered a predominant feature of PCOS and is commonly coupled with impaired fertility (41, 42). This excess of androgens is even considered a potential causative factor of PCOS as anti-androgen flutamide treatment restores cycle irregularity and ovulation in PCOS patients and in a PCOS mouse model (43, 44). The Rotterdam criteria for PCOS diagnosis in women require the presence of two of the following three clinical findings: 1) hyperandrogenism, 2) ovarian dysfunction characterized by oligo- or anovulation, or 3) polycystic ovaries (3, 45). Pre- or post-natal exposure of rodents to androgens are known to induce PCOS-like phenotype that recapitulates all 3 criteria (for

Author Manuscript Author Manuscript Author Manuscript Author Manuscript

review: 23, 24). Mouse models for exogenous exposure to androgens and patients with hyperandrogenism caused by either congenital adrenal hyperplasia or testosterone treatments develop polycystic ovaries (23). On the contrary, while NR5A1+ mice were hyperandrogenic and had impaired fertility, there was no accumulation of antral follicles and appearance of polycystic ovaries. Instead, there was accumulation of corpora lutea and appearance of retained oocytes surrounded by luteinized granulosa cells. It is possible that the relatively late and progressive increase in androgens levels, after 3m of age, leads to a different phenotype than the rodent PCOS models with pre/post-natal androgen exposure. Another possibility could be that the ovarian phenotype is at least partially driven by a direct action of NR5A1 in granulosa cells. Indeed, beyond its role as a key transcriptional regulator for steroidogenic enzymes, NR5A1 also acts as co-transcription factor for other genes in granulosa cells (46). NR5A1 is required for proper function of granulosa cells during folliculogenesis and its conditional loss specifically in granulosa cells results in infertility, abnormal estrus cycles and absence of corpora lutea (16, 17). It is therefore possible that NR5A1 overexpression in granulosa cells alters their function independent of the hyperandrogenism. For instance, NR5A1 overexpression leads to strong downregulation of both *Inhba* and *Inhbb* in the ovary. The similarities in phenotype between our model of NR5A1+ overexpression and *Inhba*/*Inhbb* conditional KO in the ovary, with defects in CL structural regression as well as presence of retained oocytes surrounded by luteinized granulosa cells (22) suggests that similar pathways are at play and low levels of Activins contribute to this ovarian phenotype.

NR5A1+ females showed some difference in timing of phenotype progression and in phenotype severity. For instance, some females became infertile by 4m of age while others remained fertile at 9m of age. We suspect that this difference is the result of variation in transgene activation. Indeed, not all granulosa cells and theca cell expressed the transgene. This is in contrast with other mouse models we and others previously developed using Nr5a1-Cre, which resulted in 100% recombination in somatic cells of the fetal gonads (20, 27–30).

Finally, both reproductive and metabolic defects could be the results of extragonadal action of androgens on the neuroendocrine system. Neuronal-specific knockout of AR protects against development of PCOS characteristics in mice exposed to androgens (36). In addition to being a target of hyperandrogenism, the development and functions of pituitary and hypothalamus depend on NR5A1 itself. Without *Nr5a1*, gonadotropes in the mouse pituitary failed to be produced and the function of hypothalamus is impaired (7, 8, 47, 48). Expression of NR5A1 in the hypothalamus is restricted to the ventromedial hypothalamic nucleus, which regulates body weight homeostasis. Interestingly, loss of *Nr5a1* alters the cellular topography within and around the ventromedial hypothalamic nucleus, and results in obesity, a phenotype similar to that of mice with lesions in the ventromedial hypothalamic nucleus (49–51). Moreover, conditional KO of *Nr5a1* in the hypothalamus impairs female reproductive functions, including irregular estrous cycles and impaired expression of steroid receptors near the ventromedial hypothalamic nucleus (52). All these findings suggest that NR5A1 in the hypothalamus is required for both reproductive and metabolic functions. Our mouse model targets cells that normally express NR5A1, which can be found in the ovary, pituitary and hypothalamus. While we did not detect significant changes in expression of

Author Manuscript Author Manuscript Author Manuscript Author Manuscript

genes involved in hypothalamic functions, it remains possible that overexpression of NR5A1 in the ventromedial hypothalamic nucleus impairs neuro-endocrine functions and contributes to both reproductive and metabolic phenotypes. Despite no clear pituitary and hypothalamus phenotype, the reproductive and metabolic defects observed in our mouse model could be the result of compound effects on the finetuned signaling between gonads and the central nervous system. The development of organ-specific models for NR5A1 over-expression would help deciphering the specific effects of NR5A1 activation within each compartment of the hypothalamic-pituitary-gonad axis.

In summary, we explored the effects of constitutive overexpression of NR5A1 in NR5A1+ cells in female mice. Overexpression of NR5A1 disrupted female fertility and metabolism, highlighting the importance of a fine-tuned control of NR5A1 in female reproductive function and regulation of body weight homeostasis. This NR5A1 overexpression mouse provides a novel model for studying not only the molecular actions of NR5A1, but also the crosstalk between endocrine, reproductive and metabolic systems.

Supplementary Material

Refer to Web version on PubMed Central for supplementary material.

Acknowledgements

This research was supported by the Intramural Research Program (Z01ES102965 to HHCY) of the NIH, National Institute of Environmental Health Sciences, and by NIH grant T32 ES007326 (to SR and JAF). We thank the late Dr. Keith Parker (UT Southwestern Medical Center) for the *Nr5a1*-Cre mice, Dr. Francesco J. DeMayo (NIEHS/NIH) for the Rosa26-LSL-*Nr5a1* mice and Ken Morohashi (Kyushu University, Japan) for the NR5A1 antibody. We are grateful to the NIEHS Comparative Medicine Branch for mouse colony maintenance and body composition analysis, the NIEHS Cellular and Molecular Pathology Branch, Pathology Image Analysis Group for histological imaging and Clinical Pathology Group for clinical chemistry assays. We also thank the Pharmacology Department at University of Eastern Finland for the LC-MS/MS measurements and the University of Virginia Center for Research in Reproduction Ligand Assay and Analysis Core, which is supported by the Eunice Kennedy Shriver NICHD/NIH Grant R24HD102061.

Nonstandard abbreviations:

NR5A1	nuclear receptor subfamily 5 group A member 1
PCOS	polycystic ovarian syndrome
MOF	multi-oocyte follicles
CL	corpora lutea
LH	luteinizing hormone
FSH	follicle-stimulating hormone
LC-MS/MS	liquid Chromatography with tandem mass spectrometry
ALP	alkaline phosphatase
AST	aspartate aminotransferase

Author Manuscript Author Manuscript Author Manuscript Author Manuscript

ALT	alanine aminotransferase
TBA	total bile acid
HDL	high-density lipoprotein
LDL	low-density lipoprotein
SEM	standard error of the mean
AR	androgen receptor
ER	estrogen receptor
DHT	dihydrotestosterone

References

1. Bozdag G, Mumusoglu S, Zengin D, Karabulut E, and Yildiz BO (2016) The prevalence and phenotypic features of polycystic ovary syndrome: a systematic review and meta-analysis. Hum Reprod 31, 2841–2855 [PubMed: 27664216]
2. Azziz R, Carmina E, Chen Z, Dunaif A, Laven JSE, Legro RS, Lizneva D, Natterson-Horowtiz B, Teede HJ, and Yildiz BO (2016) Polycystic ovary syndrome. Nature Reviews Disease Primers 2, 16057
3. Teede HJ, Misso ML, Costello MF, Dokras A, Laven J, Moran L, Piltonen T, Norman RJ, and International PN (2018) Recommendations from the international evidence-based guideline for the assessment and management of polycystic ovary syndrome†‡. Human Reproduction 33, 1602–1618 [PubMed: 30052961]
4. Lala DS, Rice DA, and Parker KL (1992) Steroidogenic factor I, a key regulator of steroidogenic enzyme expression, is the mouse homolog of fushi tarazu-factor I. Mol Endocrinol 6, 1249–1258 [PubMed: 1406703]
5. Morohashi K, Honda S, Inomata Y, Handa H, and Omura T (1992) A common trans-acting factor, Ad4-binding protein, to the promoters of steroidogenic P-450s. J Biol Chem 267, 17913–17919 [PubMed: 1517227]
6. Luo X, Ikeda Y, and Parker KL (1994) A cell-specific nuclear receptor is essential for adrenal and gonadal development and sexual differentiation. Cell 77, 481–490 [PubMed: 8187173]
7. Luo X, Ikeda Y, and Parker KL (1995) The cell-specific nuclear receptor steroidogenic factor 1 plays multiple roles in reproductive function. Philos Trans R Soc Lond B Biol Sci 350, 279–283 [PubMed: 8570692]
8. Ingraham HA, Lala DS, Ikeda Y, Luo X, Shen WH, Nachtigal MW, Abbud R, Nilson JH, and Parker KL (1994) The nuclear receptor steroidogenic factor 1 acts at multiple levels of the reproductive axis. Genes Dev 8, 2302–2312 [PubMed: 7958897]
9. Ikeda Y, Shen WH, Ingraham HA, and Parker KL (1994) Developmental expression of mouse steroidogenic factor-1, an essential regulator of the steroid hydroxylases. Mol Endocrinol 8, 654–662 [PubMed: 8058073]
10. Sekido R, and Lovell-Badge R (2008) Sex determination involves synergistic action of SRY and SF1 on a specific Sox9 enhancer. Nature 453, 930–934 [PubMed: 18454134]
11. Buaas FW, Gardiner JR, Clayton S, Val P, and Swain A (2012) In vivo evidence for the crucial role of SF1 in steroid-producing cells of the testis, ovary and adrenal gland. Development 139, 4561–4570 [PubMed: 23136395]
12. Hinshelwood MM, Repa JJ, Shelton JM, Richardson JA, Mangelsdorf DJ, and Mendelson CR (2003) Expression of LRH-1 and SF-1 in the mouse ovary: localization in different cell types correlates with differing function. Mol Cell Endocrinol 207, 39–45 [PubMed: 12972182]
13. Domenice S, Machado AZ, Ferreira FM, Ferraz-de-Souza B, Lerario AM, Lin L, Nishi MY, Gomes NL, da Silva TE, Silva RB, Correa RV, Montenegro LR, Narciso A, Costa EMF,

Author Manuscript Author Manuscript Author Manuscript Author Manuscript

Achermann JC, and Mendonca BB (2016) Wide spectrum of NR5A1-related phenotypes in 46,XY and 46,XX individuals. Birth Defects Res C Embryo Today 108, 309–320 [PubMed: 28033660]

14. Bashamboo A, Donohoue PA, Vilain E, Rojo S, Calvel P, Seneviratne SN, Buonocore F, Barseghyan H, Bingham N, Rosenfeld JA, Mulukutla SN, Jain M, Burrage L, Dhar S, Balasubramanyam A, Lee B, Members of UDN, Dumargne M-C, Eozenou C, Suntharalingham JP, de Silva KSH, Lin L, Bignon-Topalovic J, Poulat F, Lagos CF, McElreavey K, and Achermann JC (2016) A recurrent p.Arg92Trp variant in steroidogenic factor-1 (NR5A1) can act as a molecular switch in human sex development. Human Molecular Genetics 25, 3446–3453 [PubMed: 27378692]
15. Lourenço D, Brauner R, Lin L, De Perdigo A, Weryha G, Muresan M, Boudjenah R, Guerra-Junior G, Maciel-Guerra AT, Achermann JC, McElreavey K, and Bashamboo A (2009) Mutations in NR5A1 associated with ovarian insufficiency. N Engl J Med 360, 1200–1210 [PubMed: 19246354]
16. Jeyasuria P, Ikeda Y, Jamin SP, Zhao L, De Rooij DG, Themmen AP, Behringer RR, and Parker KL (2004) Cell-specific knockout of steroidogenic factor 1 reveals its essential roles in gonadal function. Mol Endocrinol 18, 1610–1619 [PubMed: 15118069]
17. Pelusi C, Ikeda Y, Zubair M, and Parker KL (2008) Impaired follicle development and infertility in female mice lacking steroidogenic factor 1 in ovarian granulosa cells. Biol Reprod 79, 1074–1083 [PubMed: 18703422]
18. Vasquez YM, Wu SP, Anderson ML, Hawkins SM, Creighton CJ, Ray M, Tsai SY, Tsai MJ, Lydon JP, and DeMayo FJ (2016) Endometrial Expression of Steroidogenic Factor 1 Promotes Cystic Glandular Morphogenesis. Mol Endocrinol 30, 518–532 [PubMed: 27018534]
19. Wu SP, Lee DK, Demayo FJ, Tsai SY, and Tsai MJ (2010) Generation of ES cells for conditional expression of nuclear receptors and coregulators in vivo. Mol Endocrinol 24, 1297–1304 [PubMed: 20382891]
20. Bingham NC, Verma-Kurvari S, Parada LF, and Parker KL (2006) Development of a steroidogenic factor 1/Cre transgenic mouse line. Genesis 44, 419–424 [PubMed: 16937416]
21. Rattan S, Brehm E, Gao L, Niermann S, and Flaws JA (2018) Prenatal exposure to di(2-ethylhexyl) phthalate disrupts ovarian function in a transgenerational manner in female mice. Biol Reprod 98, 130–145 [PubMed: 29165555]
22. Pangas SA, Jorgez CJ, Tran M, Agno J, Li X, Brown CW, Kumar TR, and Matzuk MM (2007) Intraovarian activins are required for female fertility. Mol Endocrinol 21, 2458–2471 [PubMed: 17609433]
23. Walters KA, Paris VR, Aflatounian A, and Handelsman DJ (2019) Androgens and ovarian function: translation from basic discovery research to clinical impact. Journal of Endocrinology 242, R23
24. Stener-Victorin E, Padmanabhan V, Walters KA, Campbell RE, Benrick A, Giacobini P, Dumesic DA, and Abbott DH (2020) Animal models to understand the etiology and pathophysiology of polycystic ovary syndrome. Endocrine Reviews 41, 538–576
25. Domenice S, Machado AZ, Ferreira FM, Ferraz-de-Souza B, Lerario AM, Lin L, Nishi MY, Gomes NL, da Silva TE, Silva RB, Correa RV, Montenegro LR, Narciso A, Costa EM, Achermann JC, and Mendonca BB Wide spectrum of NR5A1-related phenotypes in 46,XY and 46,XX individuals.
26. Baetens D, Stoop H, Peelman F, Todeschini A-L, Rosseel T, Coppieters F, Veitia RA, Looijenga LHJ, De Baere E, and Cools M (2017) NR5A1 is a novel disease gene for 46,XX testicular and ovotesticular disorders of sex development. Genetics in Medicine 19, 367–376 [PubMed: 27490115]
27. Lavery R, Lardenois A, Ranc-Jianmotamedi F, Pauper E, Gregoire EP, Vigier C, Moreilhon C, Primig M, and Chaboissier MC (2011) XY Sox9 embryonic loss-of-function mouse mutants show complete sex reversal and produce partially fertile XY oocytes. Dev Biol 354, 111–122 [PubMed: 21466799]
28. Nicol B, Grimm SA, Chalmel F, Lecluze E, Pannetier M, Pailhoux E, Dupin-De-Beyssat E, Guiguen Y, Capel B, and Yao HH (2019) RUNX1 maintains the identity of the fetal ovary through an interplay with FOXL2. Nat Commun 10, 5116 [PubMed: 31712577]

Author Manuscript Author Manuscript Author Manuscript Author Manuscript

29. Nicol B, Grimm SA, Gruzdev A, Scott GJ, Ray MK, and Yao HH (2018) Genome-wide identification of FOXL2 binding and characterization of FOXL2 feminizing action in the fetal gonads. Hum Mol Genet 27, 4273–4287 [PubMed: 30212841]
30. Nicol B, and Yao HH (2015) Gonadal Identity in the Absence of Pro-Testis Factor SOX9 and Pro-Ovary Factor Beta-Catenin in Mice. Biol Reprod 93, 35 [PubMed: 26108792]
31. Nomura R, Kashimada K, Suzuki H, Zhao L, Tsuji-Hosokawa A, Yagita H, Takagi M, Kanai Y, Bowles J, Koopman P, Kanai-Azuma M, and Morio T (2019) Nr5a1 suppression during the murine fetal period optimizes ovarian development by fine-tuning Notch signaling. J Cell Sci 132
32. Zhao L, Svingen T, Ng ET, and Koopman P (2015) Female-to-male sex reversal in mice caused by transgenic overexpression of Dmrt1. Development 142, 1083–1088 [PubMed: 25725066]
33. Walters KA, Gilchrist RB, Ledger WL, Teede HJ, Handelsman DJ, and Campbell RE (2018) New Perspectives on the Pathogenesis of PCOS: Neuroendocrine Origins. Trends Endocrinol Metab 29, 841–852 [PubMed: 30195991]
34. Benrick A, Chanclón B, Micallef P, Wu Y, Hadi L, Shelton JM, Stener-Victorin E, and Wernstedt Asterholm I (2017) Adiponectin protects against development of metabolic disturbances in a PCOS mouse model. Proceedings of the National Academy of Sciences 114, E7187–E7196
35. Aflatounian A, Edwards MC, Rodriguez Paris V, Bertoldo MJ, Desai R, Gilchrist RB, Ledger WL, Handelsman DJ, and Walters KA (2020) Androgen signaling pathways driving reproductive and metabolic phenotypes in a PCOS mouse model. J Endocrinol 245, 381–395 [PubMed: 32229702]
36. Caldwell ASL, Edwards MC, Desai R, Jimenez M, Gilchrist RB, Handelsman DJ, and Walters KA (2017) Neuroendocrine androgen action is a key extraovarian mediator in the development of polycystic ovary syndrome. Proc Natl Acad Sci U S A 114, E3334–e3343 [PubMed: 28320971]
37. Sugawara T, Kiriakidou M, McAllister JM, Holt JA, Arakane F, and Strauss JF 3rd. (1997) Regulation of expression of the steroidogenic acute regulatory protein (StAR) gene: a central role for steroidogenic factor 1. Steroids 62, 5–9 [PubMed: 9029708]
38. Couse JF, Yates MM, Rodriguez KF, Johnson JA, Poirier D, and Korach KS (2006) The intraovarian actions of estrogen receptor-alpha are necessary to repress the formation of morphological and functional Leydig-like cells in the female gonad. Endocrinology 147, 3666–3678 [PubMed: 16627580]
39. Wu S, Divall S, Nwaopara A, Radovick S, Wondisford F, Ko C, and Wolfe A (2014) Obesity-induced infertility and hyperandrogenism are corrected by deletion of the insulin receptor in the ovarian theca cell. Diabetes 63, 1270–1282 [PubMed: 24379345]
40. Zeng X, Xie YJ, Liu YT, Long SL, and Mo ZC (2020) Polycystic ovarian syndrome: Correlation between hyperandrogenism, insulin resistance and obesity. Clin Chim Acta 502, 214–221 [PubMed: 31733195]
41. Livadas S, Pappas C, Karachalios A, Marinakis E, Tolia N, Drakou M, Kaldrymides P, Panidis D, and Diamanti-Kandarakis E (2014) Prevalence and impact of hyperandrogenemia in 1,218 women with polycystic ovary syndrome. Endocrine 47, 631–638 [PubMed: 24752393]
42. Azziz R, Carmina E, Dewailly D, Diamanti-Kandarakis E, Escobar-Morreale HF, Futterweit W, Janssen OE, Legro RS, Norman RJ, Taylor AE, and Witchel SF (2006) Positions statement: criteria for defining polycystic ovary syndrome as a predominantly hyperandrogenic syndrome: an Androgen Excess Society guideline. J Clin Endocrinol Metab 91, 4237–4245 [PubMed: 16940456]
43. Paradisi R, Fabbri R, Battaglia C, and Venturoli S (2013) Ovulatory effects of flutamide in the polycystic ovary syndrome. Gynecological Endocrinology 29, 391–395 [PubMed: 23327685]
44. Ryan GE, Malik S, and Mellon PL (2018) Antiandrogen Treatment Ameliorates Reproductive and Metabolic Phenotypes in the Letrozole-Induced Mouse Model of PCOS. Endocrinology 159, 1734–1747 [PubMed: 29471436]
45. group, T. R. E. A. s. P. c. w. (2004) Revised 2003 consensus on diagnostic criteria and long-term health risks related to polycystic ovary syndrome (PCOS). Human Reproduction 19, 41–47 [PubMed: 14688154]
46. Jin H, Won M, Park SE, Lee S, Park M, and Bae J (2016) FOXL2 Is an Essential Activator of SF-1-Induced Transcriptional Regulation of Anti-Müllerian Hormone in Human Granulosa Cells. PLoS One 11, e0159112 [PubMed: 27414805]

Author Manuscript Author Manuscript Author Manuscript Author Manuscript

47. Ikeda Y, Luo X, Abbud R, Nilson JH, and Parker KL (1995) The nuclear receptor steroidogenic factor 1 is essential for the formation of the ventromedial hypothalamic nucleus. Mol Endocrinol 9, 478–486 [PubMed: 7659091]

48. Shinoda K, Lei H, Yoshii H, Nomura M, Nagano M, Shiba H, Sasaki H, Osawa Y, Ninomiya Y, Niwa O, and et al. (1995) Developmental defects of the ventromedial hypothalamic nucleus and pituitary gonadotroph in the Ftz-F1 disrupted mice. Dev Dyn 204, 22–29 [PubMed: 8563022]

49. Majdic G, Young M, Gomez-Sanchez E, Anderson P, Szczepaniak LS, Dobbins RL, McGarry JD, and Parker KL (2002) Knockout mice lacking steroidogenic factor 1 are a novel genetic model of hypothalamic obesity. Endocrinology 143, 607–614 [PubMed: 11796516]

50. Davis AM, Seney ML, Stallings NR, Zhao L, Parker KL, and Tobet SA (2004) Loss of steroidogenic factor 1 alters cellular topography in the mouse ventromedial nucleus of the hypothalamus. J Neurobiol 60, 424–436 [PubMed: 15307147]

51. Kim KW, Zhao L, Donato J Jr., Kohno D, Xu Y, Elias CF, Lee C, Parker KL, and Elmquist JK (2011) Steroidogenic factor 1 directs programs regulating diet-induced thermogenesis and leptin action in the ventral medial hypothalamic nucleus. Proc Natl Acad Sci U S A 108, 10673–10678 [PubMed: 21636788]

52. Kim KW, Li S, Zhao H, Peng B, Tobet SA, Elmquist JK, Parker KL, and Zhao L (2010) CNS-specific ablation of steroidogenic factor 1 results in impaired female reproductive function. Mol Endocrinol 24, 1240–1250 [PubMed: 20339005]

Author Manuscript Author Manuscript Author Manuscript Author Manuscript

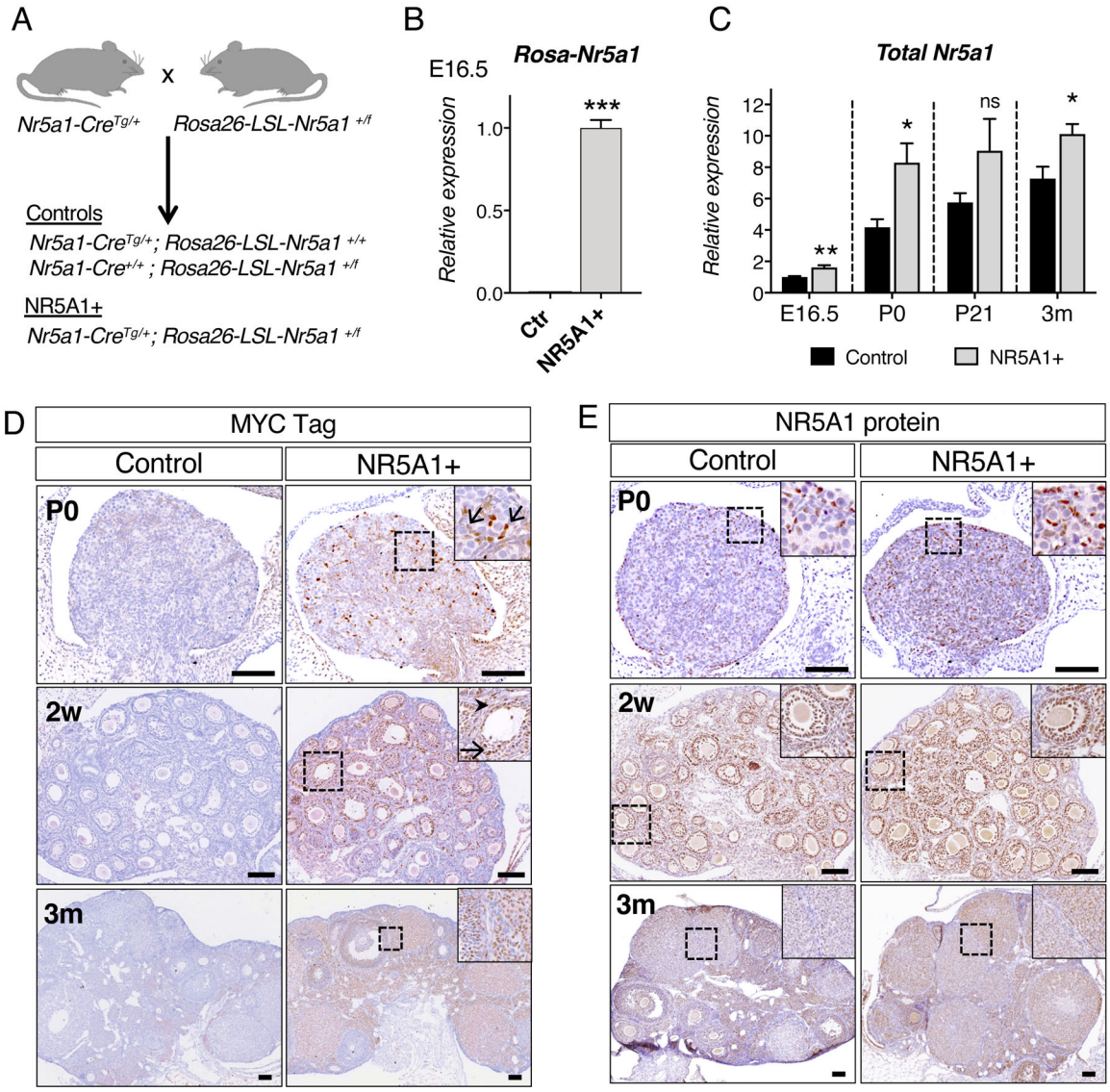

Figure 1: Constitutive induction of NR5A1 in somatic cells of the ovary.

(A) Mouse model for constitutive induction of NR5A1 in the ovarian somatic cells. The *Rosa26-LSL-Nr5a1*$^{+/f}$ mice were crossed with *Nr5a1-Cre*$^{Tg/Tg}$ mice to produce control and mutant NR5A1+ mice. (B) qPCR analysis of *Nr5a1* transgene in control and NR5A1+ ovaries at embryonic day E16.5. Bar graphs represent mean ± SEM (n=7/genotype); Student t-test ***P<0.001. (C) qPCR analysis of total *Nr5a1* (endogenous and transgene) in control and NR5A1+ ovaries at embryonic day E16.5 (n=7/genotype), birth P0 (n=6/genotype), P21 (n=4/genotype) and 3-month-old (n=4/genotype). Expression is relative to E16.5 control. Bar graphs represent mean ± SEM; Student t-test *P<0.05; **P<0.01; ns: not significant. (D-E) Immunohistochemistry for MYC-tag (D) and for NR5A1 (E) in control and NR5A1+ ovaries at birth (P0), 2 weeks (2w) and 3 months (3m) of age. Insets represent higher magnification images of the outlined areas. Arrows and arrowhead respectively indicate granulosa cells and theca cells with MYC-tag expression. Scale bar: 100 μm, n= 4 / genotype.

Author Manuscript Author Manuscript Author Manuscript Author Manuscript

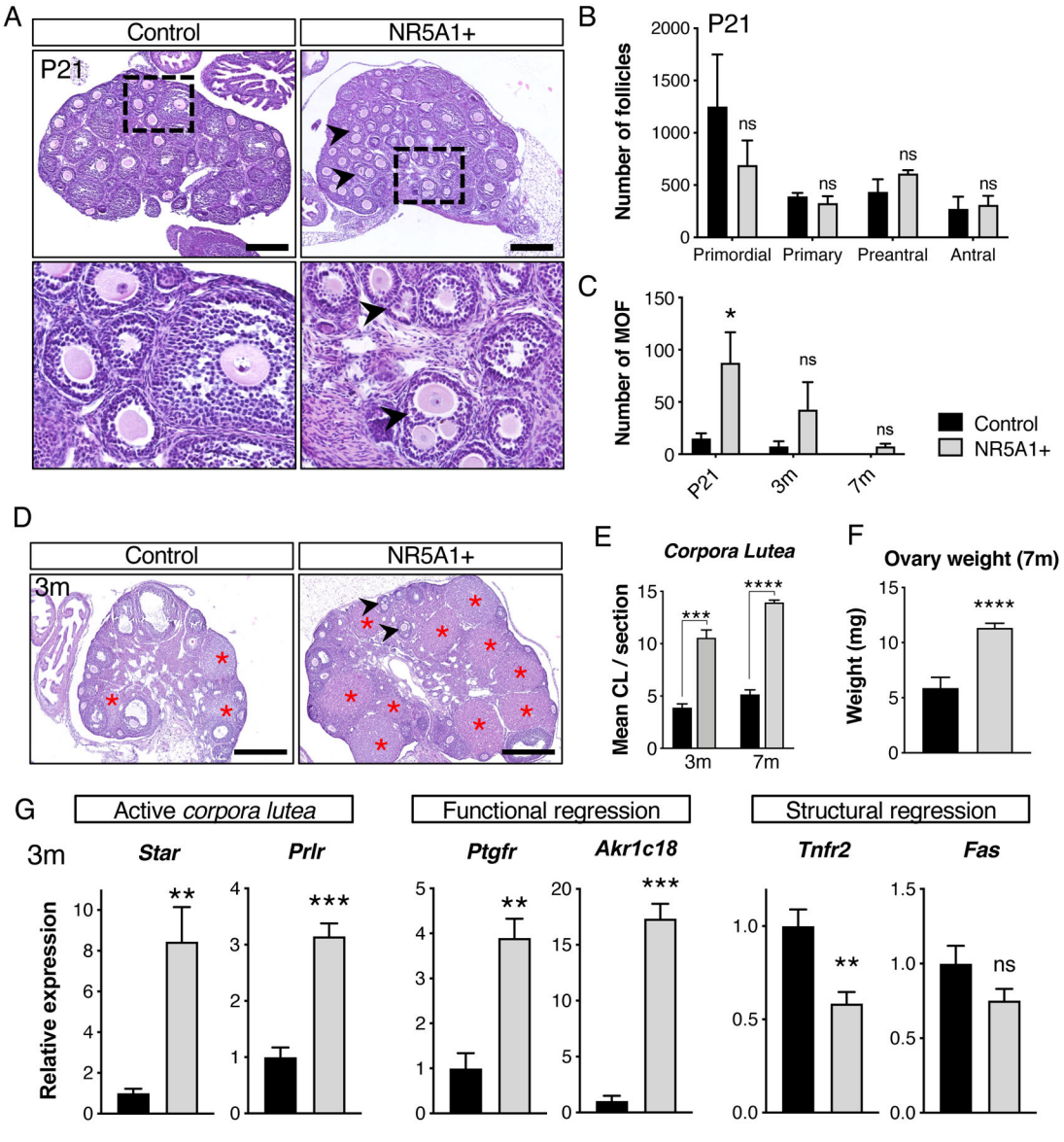

Figure 2: Overexpression of NR5A1 results in formation of multi-oocyte follicles and accumulation of corpora lutea.

(A) H&E of control and NR5A1+ ovaries at P21. Higher magnification images of the outlined areas are represented below. Arrowheads represent multi-oocyte follicles. Scale bar: 250 μm, n= 4 /genotype. (B) Quantification of primordial, primary, preantral and antral follicles in control and NR5A1+ ovaries at P21 (n=4/genotype). 2-way ANOVA test; ns: non-significant. (C) Quantification of multi-oocyte follicles (MOF) in control and NR5A1+ ovaries at P21, 3m and 7m of age (n= 4 /genotype/age). Bar graphs represent mean ± SEM; Mann-Whitney test, *P<0.05; ns: not significant. (D) H&E of control and NR5A1+ ovaries at 3m. Asterisks represent corpora lutea. Arrowheads represent multi-oocyte follicles. Scale bar: 500 μm, n= 4 /genotype. (E) Average number of corpora lutea per section in control and NR5A1+ ovaries at 3m and 7m (n= 4 / genotype). Bar graphs represent mean ± SEM; Student t-test; *** P<0.001; ****P<0.0001. (F) Weight of 7-month-old control (n=13) and NR5A1+ (n=11) ovaries. Bar graphs represent mean ± SEM; Student t-test ****P<0.0001.

Author Manuscript Author Manuscript Author Manuscript Author Manuscript

(G) qPCR analysis of genes associated with active corpora lutea, functional regression and structural regression of corpora lutea in 3-month-old ovaries. Bar graphs represent mean ± SEM (n=4 /genotype); Student t-test; ns: non-significant; **P<0.01; *** P<0.001.

Author Manuscript Author Manuscript Author Manuscript Author Manuscript

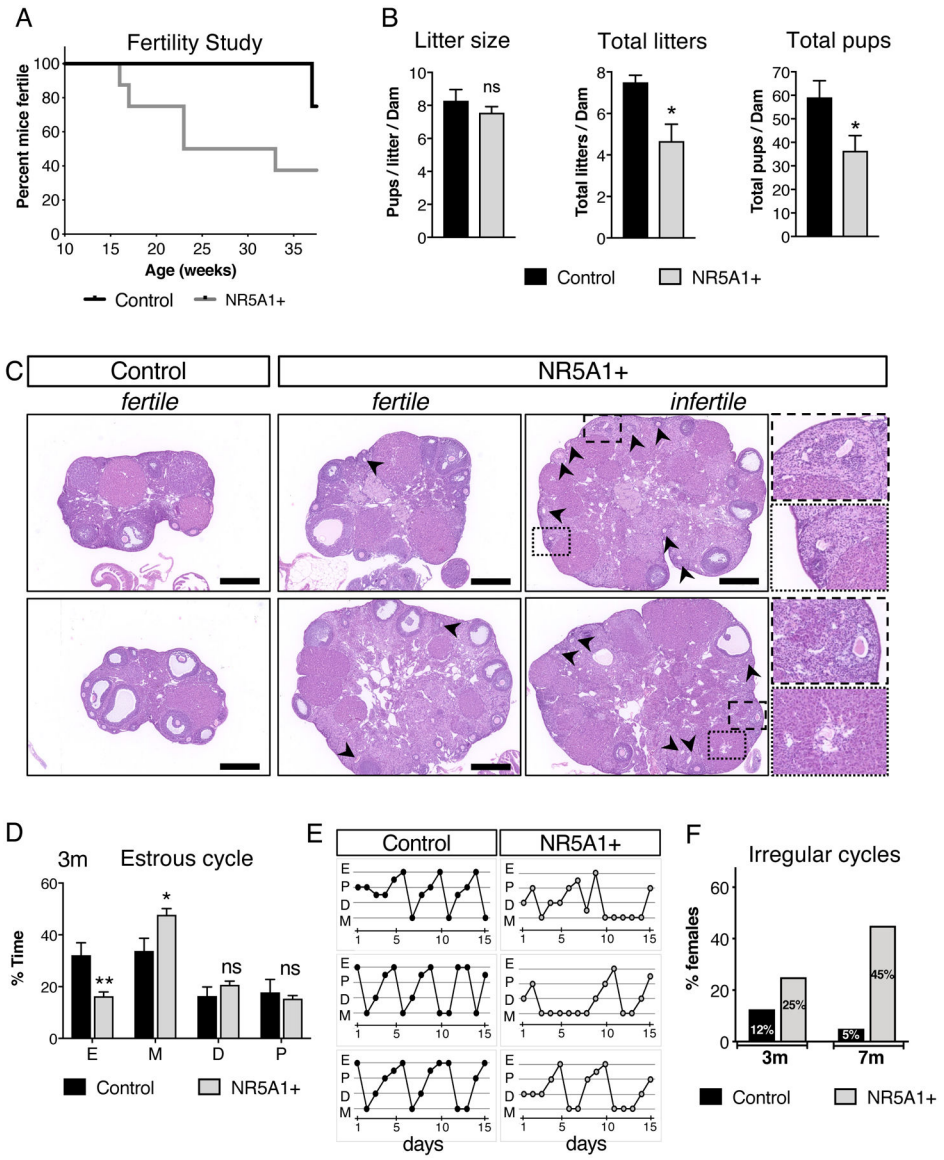

Figure 3: Overexpression of NR5A1 impairs fertility and estrous cycle.

(A) Fertility study of control (n=8) and NR5A1+ (n=9) females from 10 weeks to 38 weeks of age. The percentage of fertile females is based on the age at the time of the last litter. (B) Mean litter size, total number of litters per dam and total number of pups per dam for control (n=8) and NR5A1+ (n=9) females. Bar graphs represent mean ± SEM; Student t-test, *P<0.05; ns: not significant. (C) H&E of ovaries collected the end of the fertility study. Arrowheads and outlined area indicate retained oocytes surrounded by luteinized cells. Insets represent higher magnification images of the outlined areas. Scale bar: 500 μm. (D) Analysis of estrous cycle in control (n=9) and NR5A1+ (n=8) females at 3m of age. E: Estrus; M: Metestrus; D: Diestrus; P: Proestrus. Bar graphs represent mean ± SEM; 2-way ANOVA; *P<0.05; **P<0.01; ns: not significant. (E) Representative examples of estrous cycle of 3-month-old control and NR5A1+ females over a period of 15 days. (F) Percentage of females with irregular cycles at 3m and 7m of age for control and NR5A1+ females

Author Manuscript Author Manuscript Author Manuscript Author Manuscript

(n=8–9/genotype). Females were considered not cycling regularly if they had less than 2 cycles over a period of 15 days.

Author Manuscript Author Manuscript Author Manuscript Author Manuscript

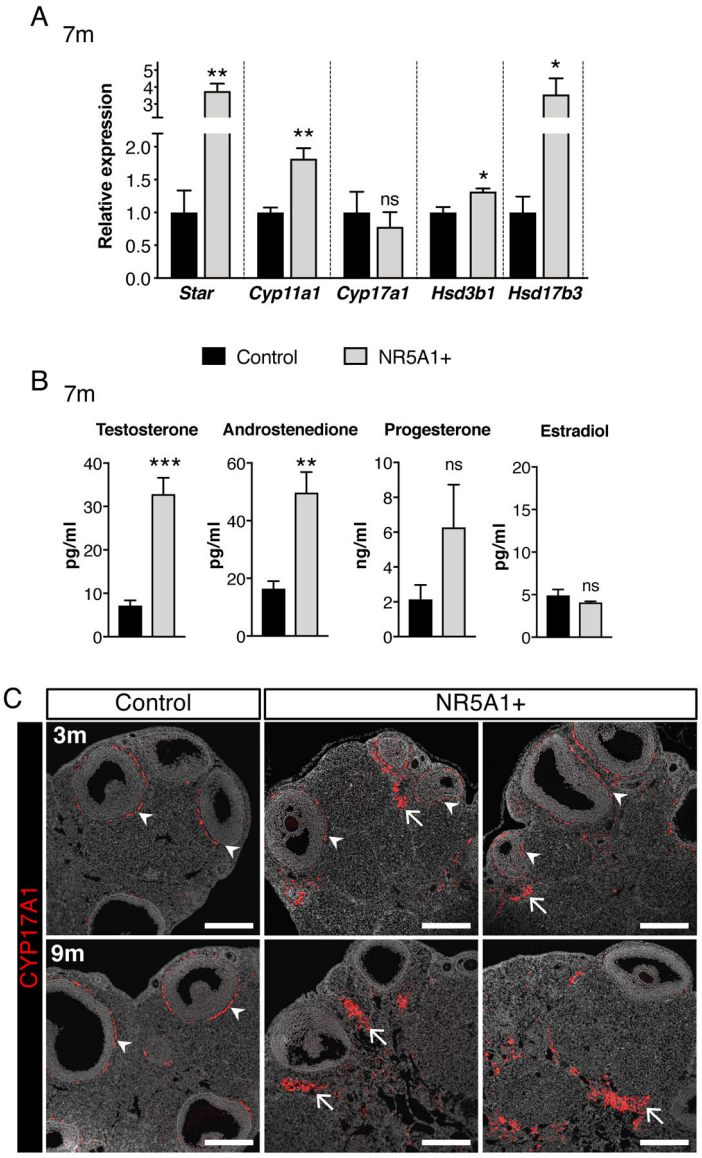

Figure 4: Overexpression of NR5A1 leads to hyperandrogenism.

(A) qPCR analysis of steroidogenic genes in 7-month-old control and NR5A1+ ovaries in metestrus. Bar graphs represent mean ± SEM (n=5/genotype); Student t-test; ns: non-significant; *P<0.05, **P<0.01. (B) LC-MS/MS analysis of hormone serum levels in 7-month-old control and NR5A1+ females in metestrus. Bar graphs represent mean ± SEM (n=6/genotype); Mann-Whitney test; **P<0.01; ***P<0.001; ns: not significant. (C) Immunofluorescence for CYP17A1 in 3- and 9-month-old control and NR5A1+ ovaries. Arrowheads show CYP17A1+ theca cells, arrows show CYP17A1+ interstitial cells. Scale bar: 250 μm.

Author Manuscript Author Manuscript Author Manuscript Author Manuscript

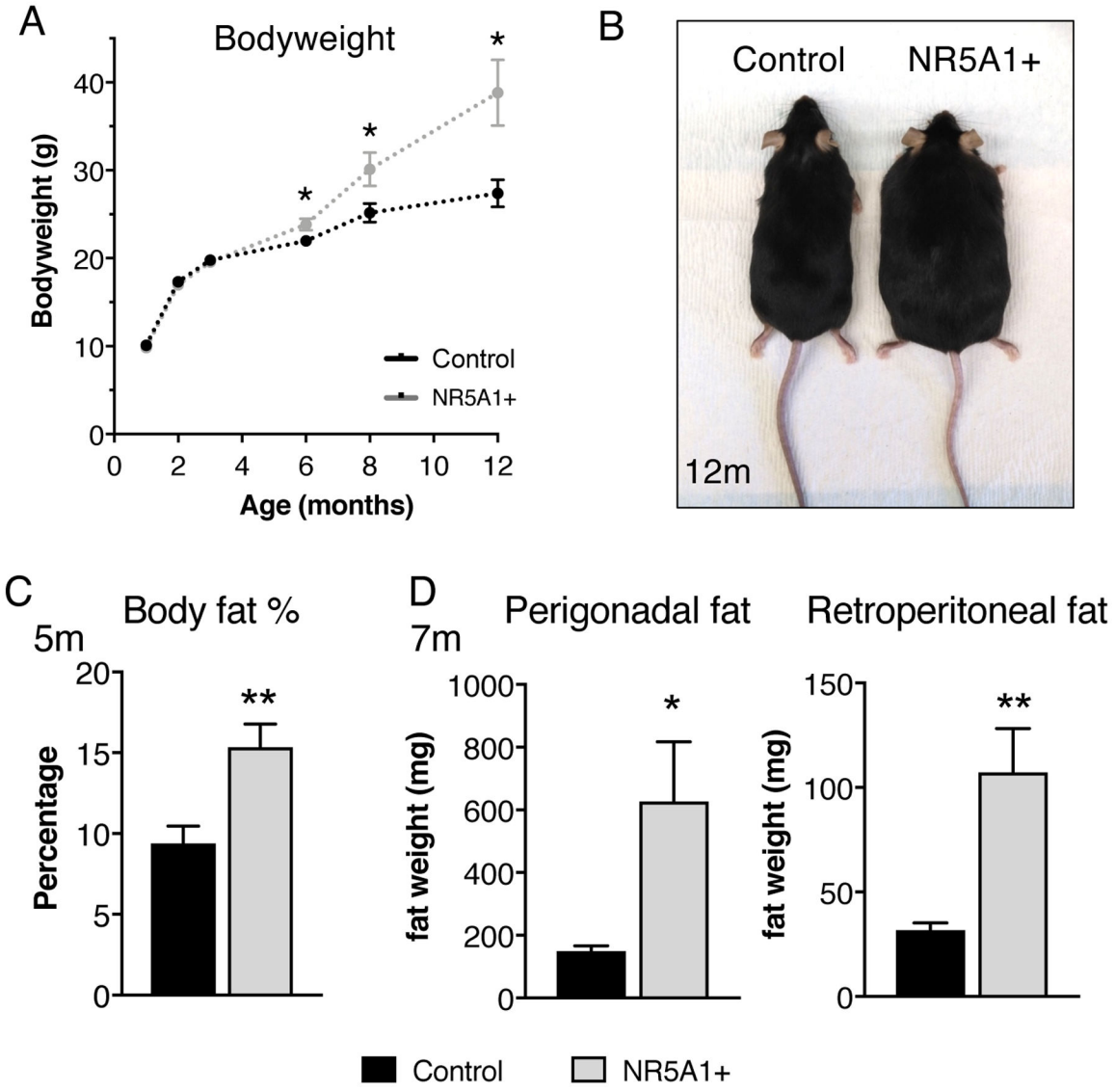

Figure 5: NR5A1+ females are overweight.

(A) Body weight of control and NR5A1+ females from 1m to 12m of age. Each time point is represented by mean ± SEM (n=10–16/genotype); Student t-test; *P<0.05. (B) Representative image of control and NR5A1+ females at 12m of age. (C) Percentage of body fat measured MRI-based device LF90 MiniSpec in control and NR5A1+ females at 5m. Bar graphs represent mean ± SEM (n=8/genotype); Student t-test; **P<0.01. (D) Perigonadal and retroperitoneal fat weight in control and NR5A1+ females at 7m. Bar graphs represent mean ± SEM (n=16/genotype); Student t-test; *P<0.05; ***P<0.001.

Author Manuscript Author Manuscript Author Manuscript Author Manuscript

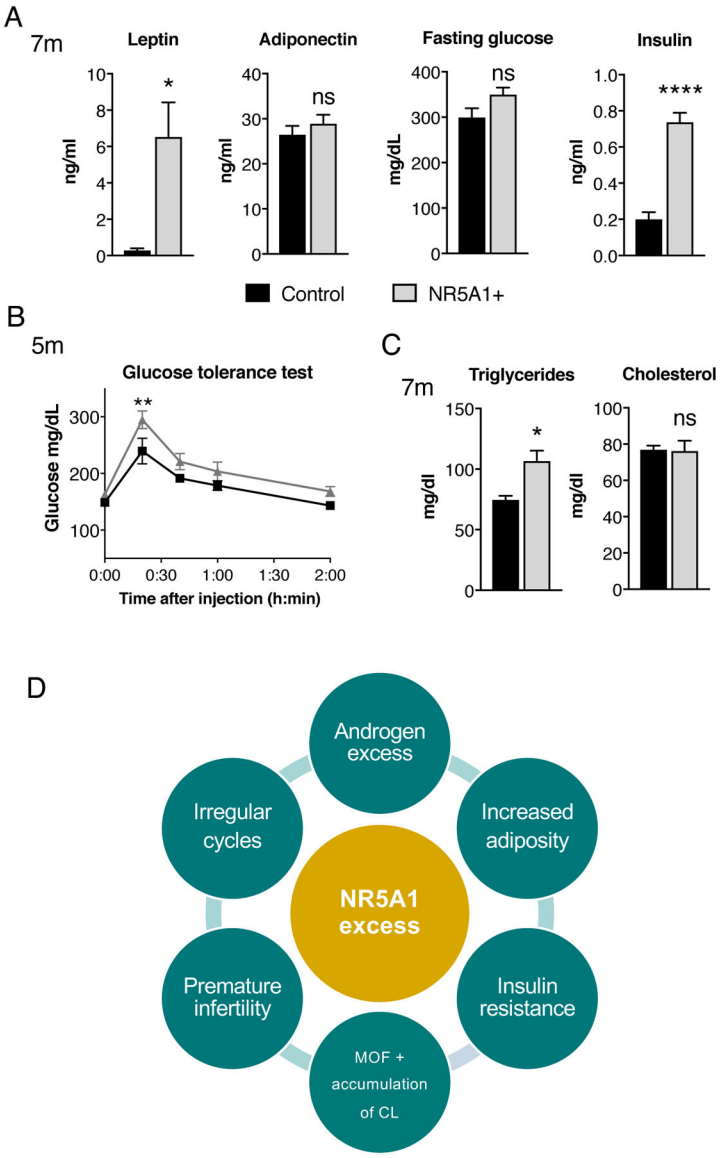

Figure 6: NR5A1+ females present metabolic defects.

(A) Fasting serum levels of leptin, adiponectin, insulin and glucose in control and NR5A1+ females at 7m. Each bar is represented by mean ± SEM (n=6/genotype); Student t-test; ns: non-significant *P<0.05, ****P<0.0001. (B) Glucose tolerance test of control (n=8) and NR5A1+ (n=9) females at 5m. Each time point is represented by mean ± SEM; 2-way ANOVA; **P<0.01. For all graphs, controls data are represented in black color and NR5A1+ data are represented in gray. (C) Fasting serum levels of Triglycerides and Cholesterol in control and NR5A1+ females at 7m. Each bar is represented by mean ± SEM (n=6/genotype); Student t-test; ns: non-significant *P<0.05. (D) Summary of the phenotypes resulting from excess NR5A1 expression in female mice.